Study of an upwelling event in the Portuguese coast

Upwelling Filaments in Aveiro region

Paulo Filipe Alexandre Correia

paulofilipe@tecnico.ulisboa.pt

Instituto Superior Técnico, Universidade de Lisboa, Av. Rovisco Pais, 1049-001 Lisboa, Portugal

Abstract

This work is about coastal upwelling in the region of Aveiro, aiming to understand and simulate the generation of filaments during an upwelling event in the summer of 2011. This region is well-known for the formation and development of these type of hydrodynamic structures and also presents some interesting topographic features, such as, the canyon of Aveiro. The main issue addressed is whether the existence of the Western Iberian Buoyant Plume (WIBP) due to river discharges, affects the formation of the so-called Aveiro filament. To verify the influence of the plume on the filament formation, numerical simulations were performed using the hydrodynamic 3D model MOHID, in two distinct scenarios. In the first scenario, the model was initialized with the known values of temperature and salinity, whereas in the second scenario the coastal fresher water was replaced by saltwater with a salinity equal to 35.9 psu. The results obtained for the first scenario show a good correlation with the ARGO buoys, and the MOHID model even performed better than the MERCATOR model. Comparing both scenarios, the main conclusion of this work is that the plume, considering only the contribution of the salinity, does not affect the filament extension but rather its direction, since there is a southward displacement. In terms of filament extension, MOHID model was compared with an analytical model, the Lentz's model. The comparison confirmed that the replacement of coastal fresher water by saltwater does not affect the filament extension, which is about 150 km in both cases. However, Lentz's model shows that without the salinity signature of the WIBP the buoyant plume reaches a distance of 122 km, while without the temperature signature the offshore distance is 127 km. These reductions in the filament extension were not observed with the MOHID model.

Keywords: costal upwelling, MOHID, ocean circulation, upwelling filaments, Western Iberian Buoyant Plume.

1. Introduction

In the last decades, studies have highlighted the importance of the temporal and spatial structure of upwelling to understand the high levels of productivity of coastal upwelling systems. The high levels of productivity in upwelling regions explains due to the vertical transport of nutrients to the photic layer (Coelho, Neves, Leitão, Martins, & Santos, 1999). The upwelled water is colder than surface water, more saline and rich in nutrients, such as nitrate, phosphate, and silicate resulting from the decomposition of organic material sinking from the surface. The summer upwelling events along the Portuguese coast

which have been studied in the last decades (Fiúza et al. 1982; Haynes et al.1993; Peliz et al., 2002) have shown that the sea surface temperature (SST) and chlorophyll-a ([Chl-a]) patterns are similar to those observed in other coastal upwelling regions. Another important aspect that has been studied, but practically absent in scientific literature, is the influence of terrestrial freshwater sources in the formation of filaments. In particular, for the region of Aveiro, located in the NW of the Portuguese coast, the major discharges are from rivers Douro, Minho and Mondego with the Galician Rias having a minor contribution. These freshwaters originate a low salinity water lens that extends along the Portuguese west coast as a buoyant plume, present all year around. It constitutes a recurrent pattern in most hydrographic data of the region, being known as the Western Iberia Buoyant Plume (WIBP).. This work leads to a better contribution in order to understand the knowledge about the processes that influences the development of the upwelling filaments in the Portuguese coast.

2. Literature review

2.1. Study area

In this study the observation area extends from near shore of Aveiro region to approximately 12ºW, between latitudes 40ºN and 41ºN. In this region, the shelf break is located at the 200m isobath. This isobath defines the beginning of the Aveiro Canyon, where the slope gets very steep just in a few kilometers. In the north and the southern edges of this canyon there is a persistent recurrent filament activity during upwelling events (Haynes et al.1993).

Circulation on Aveiro region

Figure 1 presents the conceptual model of Peliz et al. (2002), showing the major features of ocean circulation, offshore of Aveiro, during the upwelling season. The equatorward upwelling jets create a double-frontal system. The figure also shows the PC (yellow color), as well as an anticyclonic eddy that results from the interaction between the IPC and the upwelling jet. The hypothesis formulated in Peliz et al. (2002), is that both the anticyclonic eddy and the WIBP contribute to the offshore propagation of the upwelling filament located at the latitude of Aveiro.

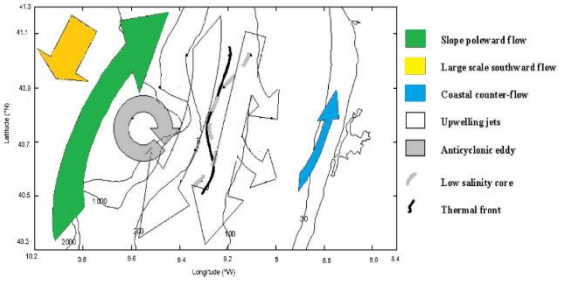

Figure 1 - Scheme circulation in study area (adapted from: Peliz et al. 2002)

2.2. Coastal upwelling in the Portuguese Coast

The coastal upwelling events exchanges water and biogeochemical properties with the offshore regions through the complex and highly dynamical Coastal Transition Zones, the core of many multidisciplinary studies in the last two decades. Most of the current studies about coastal upwelling in Western Iberia were done using satellite imagery and *in situ* data. However, some *in situ* studies that have been conducted during upwelling periods present a lack of resolution. Coastal upwelling and the outcrop of the thermocline, originates a frontal system, which is prone to the formation of several

instabilities. In the onshore region, another type of front can be formed related to gradients of salinity, when the freshwater from rivers meets the salty oceanic water.

2.2.1. Upwelling filaments

Coastal filaments are relatively narrow (typical widths of a few tens of kilometers) and shallow (usually no deeper than 150 m) stretching offshore up to several hundred kilometers from the coast. The core of a filament flows offshore with rather large velocities, usually between 0.25 and 0.5 m/s, and it is common to find onshore flows at both sides of the filament associated eddies. Filaments are frequently observed in all eastern boundary currents of subtropical gyres and are almost always associated with upwelling favourable conditions, therefore they contain relatively cold water of subsurface origin. Upwelling filaments intensify the exchange processes of biological properties in open ocean waters (Cravo et al., 2010), since their offshore transport is usually significantly larger than the Ekman transport (Kostianoy & Zatsepin, 1996). According to Ramp et al. (1991) and Strub et al. (1991), the development of filaments may result from one or a combination of several factors: baroclinic instability of the coastal current, irregularities in coastline and bottom topography, coastal divergence caused by the wind stress, and the interaction of eddies with the coastal region.

2.2.2. Influence of terrestrial freshwater sources

A significant amount of freshwater is discharged all year round to the narrow Iberian shelf by several rivers. The river runoff is mainly dependent on precipitation, therefore it changes seasonally being higher in the winter than in summer. Nevertheless, in the North coast of Portugal the major discharges are from rivers, Douro, Minho and also from the Galician Rias, that have a relevant contribution to the WIBP. According to Peliz et al., (2002), the accumulated river run-off generates a buoyant plume that extends along the coast and is present all year around, having a strong influence on shelf circulation. The WIBP is made of low salinity water (S< 35.8 psu) from winter runoff of several rivers, mentioned above, on the North coast of Portugal and Spain (Peliz et al. 2005; Peliz et al. 2002). This plume promotes a strong stratification over the shelf that reduces the thickness of the Ekman layer and the offshore Ekman transport, creating a front along the inner-shelf associated with a northward baroclinic transport.

3. Methodology

3.1. Mathematical model

The model used to the development of this work was MOHID water 3D (Braunschweig et al., 2002), which since its creation has been applied to various locations, with different conditions and for different purposes (e.g. Trancoso et al., 2005; Coelho et al., 1998). This model is built through an interconnected set of modules using object-oriented programming in FORTRAN 95, as described in Decyk (Decyk et al., 1997), each module being responsible for the management of a portion of the information, summing up a total of 40 modules developed over three decades of research work.

3.1.1. Hydrodynamic

The equations that represent this hydrodynamic model are:

$$\frac{\partial u}{\partial t} + \frac{\partial (uu)}{\partial x} + \frac{\partial (uv)}{\partial y} + \frac{\partial (uw)}{\partial z} = fv - \frac{1}{\rho_0}\frac{\partial p}{\partial x} + \frac{\partial}{\partial x}\left(v_H \frac{\partial u}{\partial x}\right) + \frac{\partial}{\partial y}\left(v_H \frac{\partial u}{\partial y}\right) + \frac{\partial}{\partial z}\left(v_v \frac{\partial u}{\partial z}\right) \quad (1)$$

$$\frac{\partial v}{\partial t} + \frac{\partial (vu)}{\partial x} + \frac{\partial (vv)}{\partial y} + \frac{\partial (vw)}{\partial z} = -fu - \frac{1}{\rho_0}\frac{\partial p}{\partial y} + \frac{\partial}{\partial x}\left(v_H \frac{\partial v}{\partial x}\right) + \frac{\partial}{\partial y}\left(v_H \frac{\partial v}{\partial y}\right) + \frac{\partial}{\partial z}\left(v_v \frac{\partial v}{\partial z}\right) \quad (2)$$

Where u, v and w are the components of the velocity vector in the x, y and z directions respectively, f is the Coriolis parameter, v_H and v_v the turbulent viscosities in the horizontal and vertical directions and p is the pressure. The turbulent viscosity is computed differently for the horizontal and vertical directions. The total pressure gradient is the sum of the gradients of atmospheric pressure, sea surface elevation (barotropic pressure gradient) and density distribution (baroclinic pressure gradient). The Hydrodynamic Model computes the advective and diffusive fluxes, the discharges of water, sediment fluxes, oxygen and heat changes with the atmosphere and sedimentation fluxes.

3.1.2. Initial conditions

With the objective to observe how the WIBP affects the filament in the Aveiro region, two simulation scenarios were performed, in order to make a comparison between them. Both simulations started on 31 May 2011, with a spin up of 5 days, until 30 August 2011. The first scenario consisted of performing the simulation using the PCOMS model and in the second scenario the initial conditions where changed, removing all the salinity values bellow 35.9 psu, from the Mercator file (Figure 2). Although, the literature reports a salinity value between 35.7 and 35.8, for WIBP, the value of 35.9 was chosen due to numerical stability reasons.

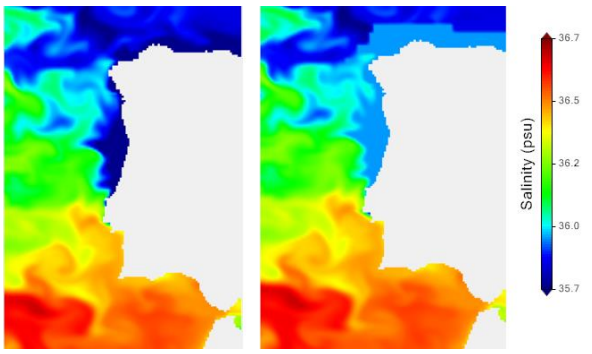

Figure 2 - Mercator initial file for scenario 1 (left) with the WIBP and for scenario 2 (right) without the WIBP.

4. Validation of the hydrodynamic model

4.1. Argo buoy

The observations of the Argo buoys found on the Portuguese coast were used for the validation of the model. In the Figure 3, it is possible to verify that the results of the MOHID baroclinic model once again, agree well with the observations and with the results of the Mercator model. Regarding temperature, both models have excellent performances with the same correlation around 1000m depth, the level of Mediterranean water. Despite the discrepancies between the Mercator model and the observations, the coefficient R= 0.998. The RMSE value is slightly higher in the MOHID model (0.241ºC) than in the Mercator (0.231ºC). Considering the bias, both models have an excellent fit against the Argo data. In relation so salinity, the results are less accurate, especially in the upper 100m, i.e., the mixed layer and

MOHID model manages to mitigate these errors and, on the whole presents better results, as can be seen from the statistical parameters.

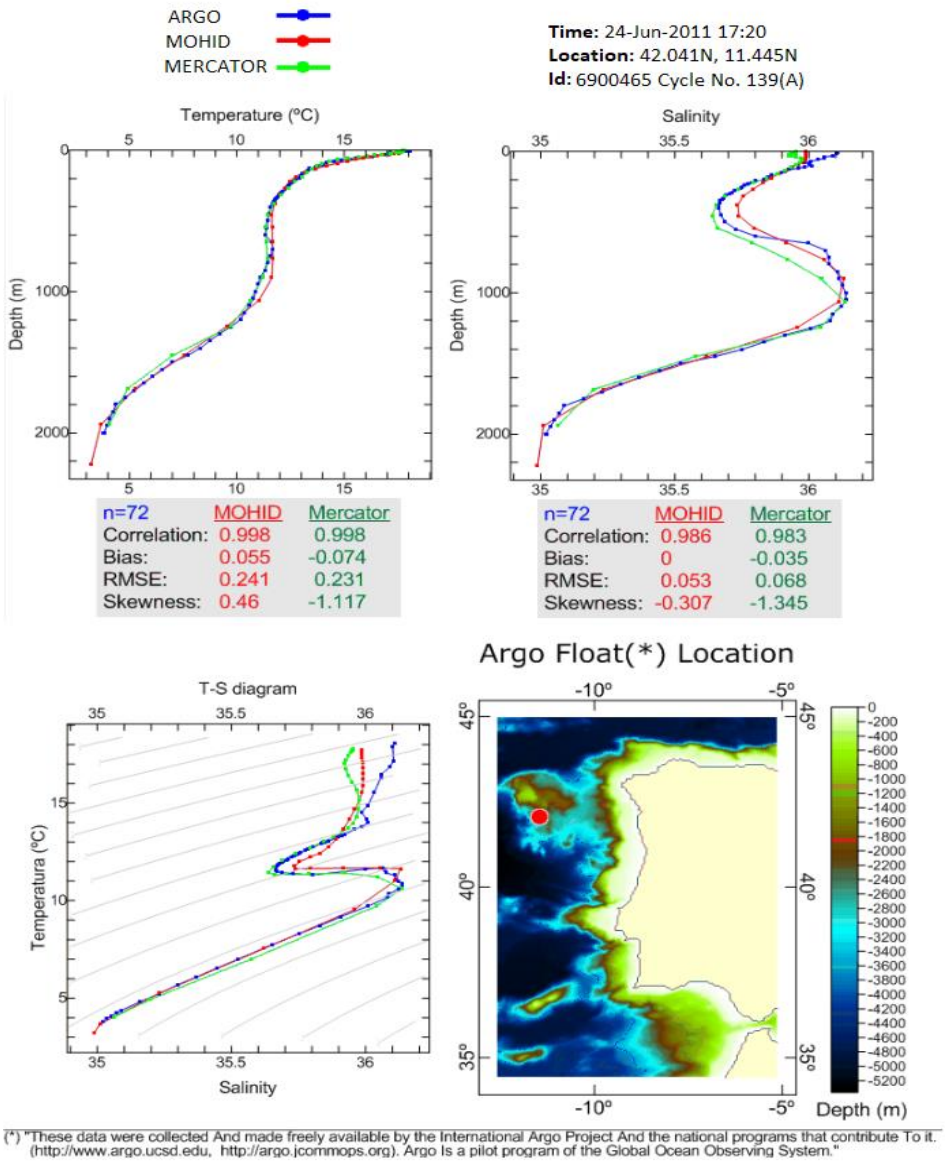

Figure 3 - Comparison between the data from MOHID model and the Argo buoys on 24 June 2011.

5. Results and discussion

5.1. SST comparison between the model results with WIBP and satellite images

The comparison of model results and satellite images are shown in Figure 4 for the period between 10 July 2011 and 25 July 2011. This period corresponds to the beginning of the upwelling event until the filament, located around 41ºN, reaches its maximum extension. In the satellite imagery of 10 July (Figure 4a), 18 July (Figure 4b) and 25 July (Figure 4c), it is possible to observe the beginning of an upwelling event, as well as the development of a filament near 41ºN. The filament is associated with a strong offshore surface current, consistent with its westward propagation, reaching approximately 150 km in length (~2º), on July 25 (Figure 4c). The lighter waters at the surface layer of the filament, are colder (~14 – 15ºC) than the surrounding waters (~16-17ºC), providing a buoyancy force that boosts its propagation.

Comparing the results of MOHID with satellite images, it is possible to conclude that it is a reliable numerical tool , being able to reproduce the development of the Aveiro filament (red rectangles in Figure 4c, Figure 4g and 5). The zooms in the region of the filament for the satellite images (Figure 4d) and model results (Figure 4h), show a good agreement in SST, as well as in the shape and extension of the filament, which reaches approximately 150 km after fifteen days of upwelling.

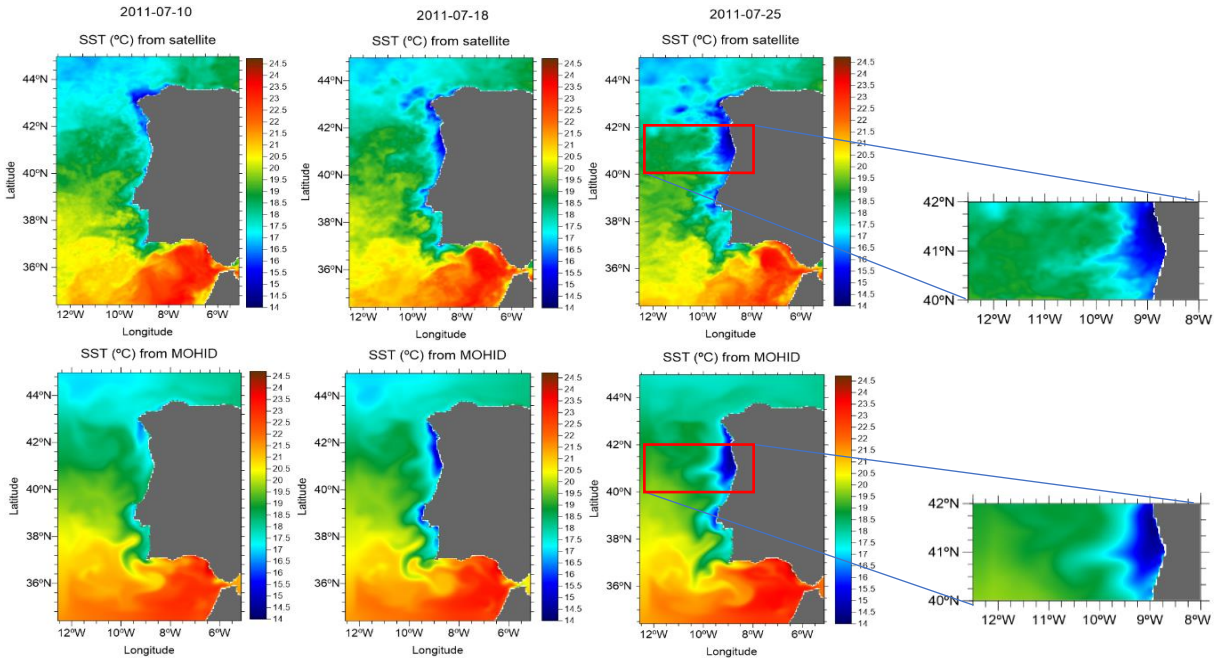

Figure 4 - SST from satellite on (a) 10 July, (b) 18 July and (c) 25 July 2011 and results from MOHID model, on (e) 10 July, (f) 18 July and (g) 25 July. On (d) and (h) is represented a zoom in the study area.

5.2. Comparison of SST results without WIBP

In order to verify the impact of the WIBP on the formation of the filament offshore near Aveiro, a second scenario of simulations were performed, removing from simulation initial conditions all the water whose salinity value was lower than 35.9 psu. Looking at the Figure *5*, which represents the filament during its maximum extension, it is evident that the change introduced in the initial conditions of salinity had a small impact on the formation of the filament, as suggested by Pelíz et al. (2002).

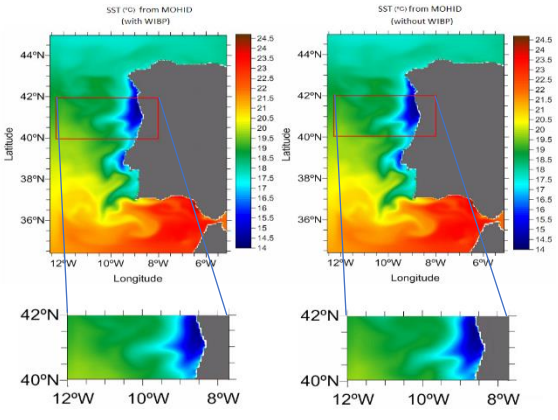

Figure 5 - SST values for MOHID, with WIBP (left) and without WIBP (right) on 25 July 2011.

5.2.2. Vertical cross-sections

In order to have a better understanding of the WIBP impact, vertical cross-sections of the flow (Figure 7) at 41ºN were also analysed, for the same period of the SST images. Figure 6 shows the SST and horizontal velocity fields obtained with the MOHID model for 25 July at 12 a.m., clearly representing a typical upwelling circulation.

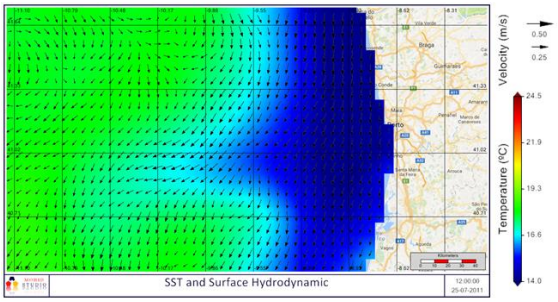

Figure 6 - SST (colours) and surface velocity fields (arrows) obtained with the MOHID model with WIBP for 25 July at 12 a.m. The yellow line represents the location of the vertical cross-section where the flow was subsequently analysed.

Figure 7 shows the alongshore velocity and density anomalies, for the section mentioned above, considering both scenarios, i.e., with and without the salinity effect of the WIBP. Typical patterns of a summer upwelling event in the western Portuguese coast are present, namely, along-shore velocities mostly negative (southward) and surface-intensified, as well as a costal counter-flow. Southward alongshore velocities range from -0.1 (Figure 7a) to -0.25 m/s at the surface (Figure 7b). In Figure 7c) it is possible to identify the double upwelling front, approximately between -9.5º and -9.7º , as mentioned by Peliz et al. (2002) in their conceptual scheme (Figure 1 in this work). Although slightly less intense than in their observations, the upwelling jet is still clearly visible. Offshore of the upwelling jet, a poleward flow is observed in Figure 7a and Figure 7c, located between -11º and -10.3º, with velocities around 0.03 m/s. This poleward flow has been documented along all eastern boundary currents and in our studied region it corresponds to the IPC, mentioned by Peliz et al. (2005) and Torres et al. (2007). Although its location changes seasonally, during a summer upwelling event it may interact with the filament, acting like a barrier that hinders its offshore advection. Otero et al. (2008), concluded that the offshore spreading of the WIBP is highly influenced by the wind regime and the mesoscale circulation (i.e. the PCC and IPC). They also concluded that the WIBP is confined at the coast when poleward winds prevail, being exported offshore and southward under upwelling favourable winds. Another study by Rossi et al. (2013) shows that the freshwater from the WIBP may be advected inside the filament as far as 140 km offshore. In addition to the previous remarks regarding the contribution of the mesoscale circulation and the WIBP to the propagation of the filament, Peliz et al. (2002) suggest that an anticyclonic eddy may be formed between the IPC and the upwelling jet, improving the offshore extension of the filament. No signs of such eddy were observed in MOHID results. The previous remarks concern the simulation with the WIBP. In what regards the impact of the WIBP, comparing Figure 7c and 27f the main conclusion is that the buoyant plume affects primarily the intensity and vertical extension of the upwelling jet, more conspicuous in the case without the salinity signature of the WIBP. A possible explanation for this is based on the fact that, without the WIBP, coastal waters become denser and, therefore, the upward slope of the isopycnals towards the shore creates a baroclinic pressure force that reinforces the southward flow. Actually, looking at Figure 7i, the green area, roughly at the same position of the core of the

upwelling jet, corresponds to denser water without WIBP.

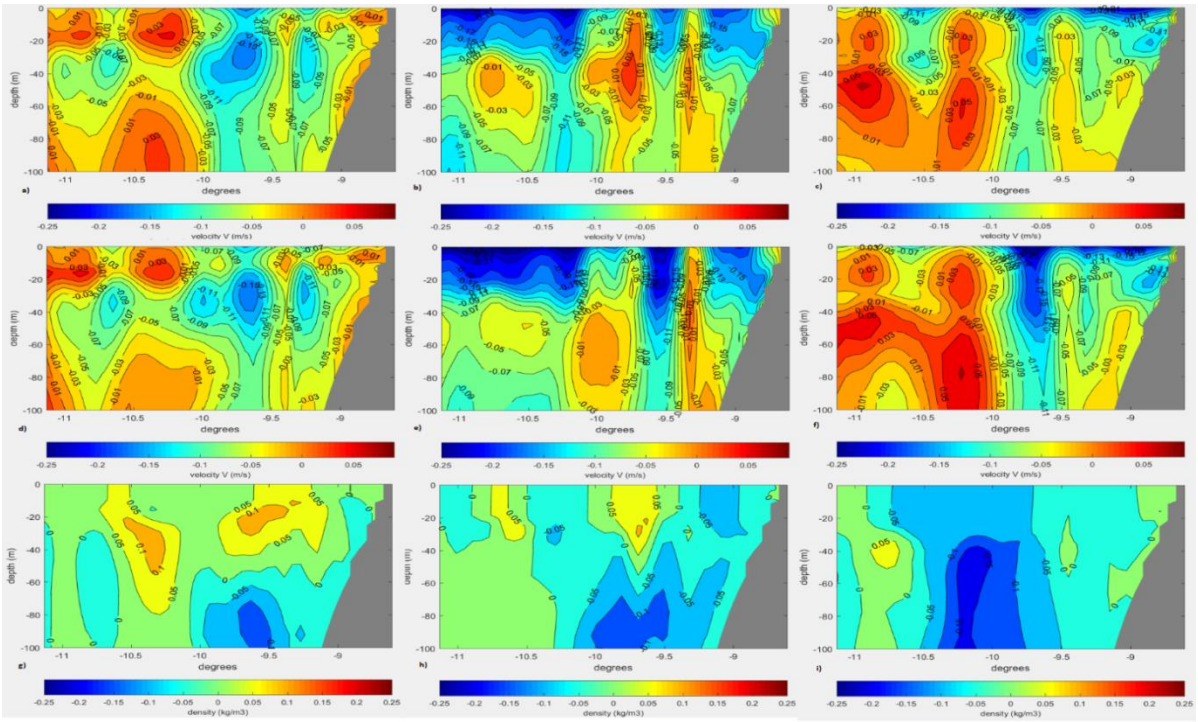

Figure 7 - Vertical cut at 41oN during the upwelling event. Images a), b), and c) presents the North (positive values) and South (negative values) velocities (with WIBP) for 10 of July, 18 of July and 25 of July 2011, respectively; Images d), e), and f) presents the along-shore velocities (without WIBP) for the same days; Images g), h), and i) presents the differences between density anomalies without and with WIBP.

5.2.3. Differences between scenarios

Figure 8 shows the difference in SST between the simulations with and without the salinity signature of the WIBP. The red and blue spots at the latitude of the Aveiro filament may be explained by its southward displacement. Superimposed to this effect, there may also be differences in the thermal gradient across the filament for the two scenarios. This subject needs further research. Another interesting observation is that changing the salinity of the WIBP also affects the filaments formation in the Cape Roca.

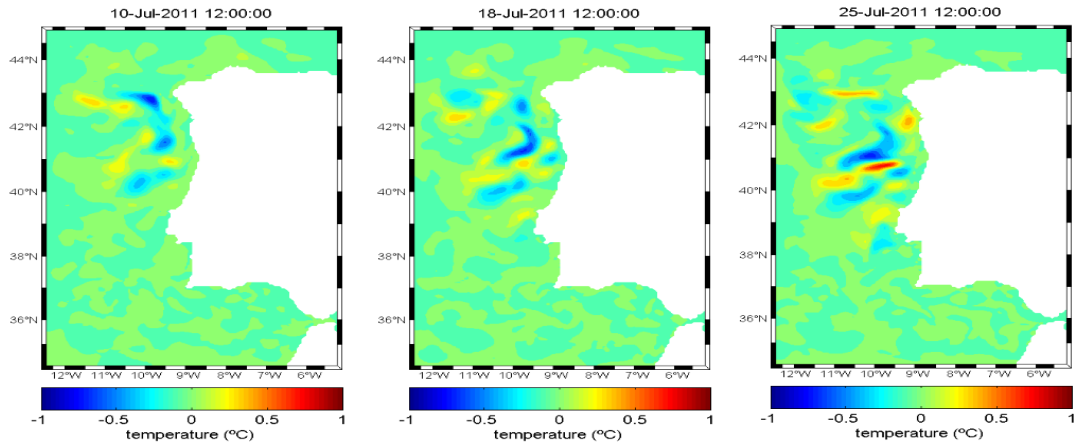

Figure 8 - Differences between SST obtained for the simulations with WIBP and without WIBP, for 10 July, 18 July and 25 July, respectively.

5.3. Comparison between MOHID model and Lentz's model

It is interesting to compare the filament extension obtained with the MOHID model, with the results of an analytical model. The model chosen was the Lentz's model (2004). Since it is two-dimensional, there are no changes along the alongshore distance, i.e., $\partial/\partial y = 0$.

Densities can be calculated using the equation of state (Cushman-Roisin, 2008):

$$\rho = \rho_0[1 - \alpha(T - T_0) + \beta(S - S_0)] \qquad (3)$$

where the constants ρ_0, T_0, S_0 are reference values of density, temperature, salinity, respectively, α is the coefficient of thermal expansion and β the coefficient of saline contraction. Typical seawater values are $\rho_0 = 1028\ kgm^{-3}$, $T_0 = 10\ ºC$, $S_0 = 0.035$, $\alpha = 1.7\times10^{-4}K^{-1}$, $\beta = 7.6\times10^{-4}$.

The input parameters used are:

$T_a = 17\ ºC$, $T_i = 19\ ºC$, $S_a = 36\ psu$, $S_i = 35.5\ psu$, $\tau^{sy} = 0.09\ Pa$, $h_i = 30\ m$, $W_i = 5\ km$.

For these values $\boldsymbol{X \approx 156\ km}$ after 15 days of upwelling, which is similar to the value obtained numerically ($\approx 150\ km$) for the offshore extension of Aveiro filament. If we consider $S_i = S_a$, keeping constant the other values, the effect of fresher water is discarded and $\boldsymbol{X \approx 122\ km}$, i.e., a reduction of 22 % in the offshore distance reached by the plume. Likewise for the temperature. If we consider $T_i = T_a$, keeping constant the other values, the effect of the temperature signature of the WIBP is no longer considered and $\boldsymbol{X \approx 127\ km}$, which represents a reduction of 19 %. These changes were not observed with the MOHID model, which means that further research is needed. It is interesting to compare the impact of the temperature and salinity signatures. From equation (21), one obtains $dS = -(\alpha/\beta)dT = -0.224dT$, for the same change in density. In other words, a decrease of 2 ºC (the difference between T_i and T_a) has an effect on density equivalent to an increase in salinity of 0.448 psu. For the present case, this means that the impact of the salinity and temperature signatures are almost equivalent, with a slightly higher contribution of

the former, as confirmed by the results of the Lentz's model.

It is important to keep in mind that Lentz's model does not simulate the generation of upwelling filaments. The existence of these hydrodynamic features requires alongshore variations of offshore propagation of coastal waters, a restriction excluded from Lentz's model since it is two-dimensional. In addition, filaments are prone to baroclinic instabilities (which explains why eddies are ubiquitous whenever filaments are present) and such instabilities are not considered in Lentz's model. However, the Aveiro upwelling filament is closely related to the offshore transport of a buoyant plume, which was the main reason for having chosen Lentz's model, despite its inaccurate description of the local hydrodynamics. In this regard, we should be aware of the fact that the offshore propagation of the Aveiro filament is counteracted by currents with a relevant meridional component, such as: the southward upwelling jets and, further offshore, the IPC and the PC. On the other hand, according to Peliz et al. (2002), the offshore propagation can be boosted by an anticyclonic eddy formed between the upwelling jet and the IPC. Neither the aforementioned currents nor the anticyclonic eddy are taken into account in Lentz's model.

6. Conclusions and future work

Despite all the difficulties, the main conclusion of this work was that the salinity signature of the WIBP does not change the extension of the Aveiro filament. However, it has a relevant impact in the filament orientation. Changing the salinity in the WIBP, intensifies the upwelling jet, which is responsible for the southward displacement of the filament. In addition, it also affects the Cape Roca filaments formation. As a future work, to gain a deeper insight into WIBP's contribution to Aveiro filament formation, it might be interesting to apply a different methodology comparing two simulations with and without the river discharges. The short time available for this work and the computational limitations have prevented this approach. The ecological implications were out of the scope of the present study, but it would also be interesting to assess the effect of the WIBP on the primary production (phytoplankton, etc.) inside the filament.

References

Braunschweig, F.; Leitao, P. C.; Fernandes, L.; Pina, P. N. (2002). The object oriented design of the integrated Water Modelling System, 1–12.

Coelho, H. S.; Neves, R. R.; Leitão, P. C.; Martins, H.; Santos, A. P. (1998). The slope current along the western European margin: A numerical investigation. *Boletin Instituto Espanol de Oceanografia*, 61–72.

Coelho, H. S., Neves, R. R., Leitão, P. C., Martins, H., & Santos, a P. (1999). The slope current along the western European margin : A numerical investigation. *Bol. Inst. Esp. Oceanogr.*, *15*(1–4), 61–72.

Cravo, A., Relvas, P., Cardeira, S., Rita, F., Madureira, M., & Sa, R. (2010). An upwelling filament off southwest Iberia : Effect on the chlorophyll a and nutrient export, *30*(October 2004), 1601–1613. https://doi.org/10.1016/j.csr.2010.06.007

Decyk, V. K.; Norton, C. D.; Szymanski, B. K. (1997). Expressing Object-Oriented Concepts in Fortran90. *ACM Fortran Forum*.

Fiúza, A. F. D., de Macedo, M. E., & Guerreiro, M. R. (1982). Climatological space and time variation of the Portuguese coastal upwelling. *Oceanologica Acta*, *5*(1), 31–40. Retrieved from http://archimer.ifremer.fr/doc/00120/23169/21014.pdf

Haynes, R., Barton, E. D., & Pilling, I. (1993). Development, persistence, and variability of upwelling filaments off the Atlantic coast of the Iberian Peninsula. *Journal of Geophysical Research*, *98*(C12), 22681. https://doi.org/10.1029/93JC02016

Kostianoy, A. G., & Zatsepin, A. G. (1996). MARINE The West African coastal upwelling filaments and cross-frontal water exchange conditioned by them, *7963*(95).

Otero, P., Ruiz-villarreal, M., & Peliz, A. (2008). Variability of river plumes off Northwest Iberia in

response to wind events, *72*, 238–255. https://doi.org/10.1016/j.jmarsys.2007.05.016

Peliz, Alvaro, Rosa, T. L., Santos, A. M. P., & Pissarra, J. L. (2002). Fronts, jets, and counter-flows in the Western Iberian upwelling system. *Journal of Marine Systems*, *35*(1–2), 61–77. https://doi.org/10.1016/S0924-7963(02)00076-3

Peliz, Á., Dubert, J., Santos, A. M. P., Oliveira, P. B., & Le Cann, B. (2005). Winter upper ocean circulation in the Western Iberian Basin - Fronts, Eddies and Poleward Flows: An overview. *Deep-Sea Research Part I: Oceanographic Research Papers*, *52*(4), 621–646. https://doi.org/10.1016/j.dsr.2004.11.005

Pelíz, Á, Rosa, T. L., Santos, a M. P., & Pissarra, J. L. (2002). Fronts, currents and couner-flows in the Western Iberian upwelling system. *Journal of Marine Systems*, *35*, 61–77. https://doi.org/10.1016/S0924-7963(02)00076-3

Ramp, S. R., Jessen, P. F., Brink, K. H., Niiler, P. P., Daggett, F. L., & Best, J. S. (1991). The Physical Structure of Cold Filaments Near Point Arena , California , During June 1987, *96*(91).

Rossi, V., Garçon, V., Tassel, J., Romagnan, J. B., Stemmann, L., Jourdin, F., … Morel, Y. (2013). Cross-shelf variability in the Iberian Peninsula Upwelling System: Impact of a mesoscale filament. *Continental Shelf Research*, *59*, 97–114. https://doi.org/10.1016/j.csr.2013.04.008

Strub, P. T. E. D., Kosro, P. M., & Huyer, A. (1991). The Nature of the Cold Filaments in the California Current System, *96*.

Torres,R.; Barton, E. (2007). Onset of the Iberian upwelling along the Galician coast. *Continental Shelf Research*, *27*, 1759–1778.

Trancoso, A. R. (2005). Modelling macroalgae using a 3D hydrodynamic-ecological model in a shallow, temperate estuary. *Ecological Modelling*, 232–246.